Accepted Manuscript

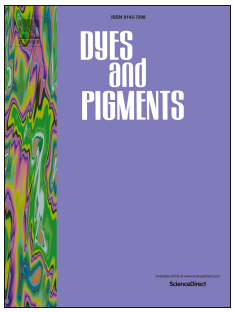

4′-phenyl-2,2':6′,2″-terpyridine derivatives-synthesis, potential application and the influence of acetylene linker on their properties

Dawid Zych, Aneta Słodek, Marek Matussek, Michał Filapek, Grażyna Szafraniec-Gorol, Sławomir Maślanka, Stanisław Krompiec, Sonia Kotowicz, Ewa Schab-Balcerzak, Karolina Smolarek, Sebastian Maćkowski, Marian Olejnik, Witold Danikiewicz

PII: S0143-7208(17)31108-7

DOI: 10.1016/j.dyepig.2017.07.030

Reference: DYPI 6119

To appear in: *Dyes and Pigments*

Received Date: 12 May 2017

Revised Date: 15 June 2017

Accepted Date: 14 July 2017

Please cite this article as: Zych D, Słodek A, Matussek M, Filapek Michał, Szafraniec-Gorol Graż, Maślanka Sł, Krompiec Stanisł, Kotowicz S, Schab-Balcerzak E, Smolarek K, Maćkowski S, Olejnik M, Danikiewicz W, 4′-phenyl-2,2':6′,2″-terpyridine derivatives-synthesis, potential application and the influence of acetylene linker on their properties, *Dyes and Pigments* (2017), doi: 10.1016/j.dyepig.2017.07.030.

4'-Phenyl-2,2':6',2''-terpyridine derivatives - synthesis, potential application and the influence of acetylene linker on their properties

Dawid Zych[a]*, Aneta Słodek[a], Marek Matussek[a], Michał Filapek[a], Grażyna Szafraniec-Gorol[a], Sławomir Maślanka[a], Stanisław Krompiec[a], Sonia Kotowicz[a], Ewa Schab-Balcerzak[a][b], Karolina Smolarek[c], Sebastian Maćkowski[c], Marian Olejnik[d], Witold Danikiewicz[d]

[a] Institute of Chemistry, Faculty of Mathematics, Physics and Chemistry, University of Silesia, Szkolna 9, 40-007 Katowice, Poland

[b] Centre of Polymer and Carbon Materials, Polish Academy of Sciences, M. Curie-Sklodowska 34, 41-819 Zabrze, Poland

[c] Institute of Physics, Faculty of Physics, Astronomy and Informatics, Nicolaus Copernicus University, Grudziadzka 5, 87-100 Torun, Poland

[d] Institute of Organic Chemistry, Polish Academy of Sciences, Kasprzaka 44/52, 01-224 Warszawa 42, Poland

*Corresponding Author: dawidzych92@gmail.com (Dawid Zych)

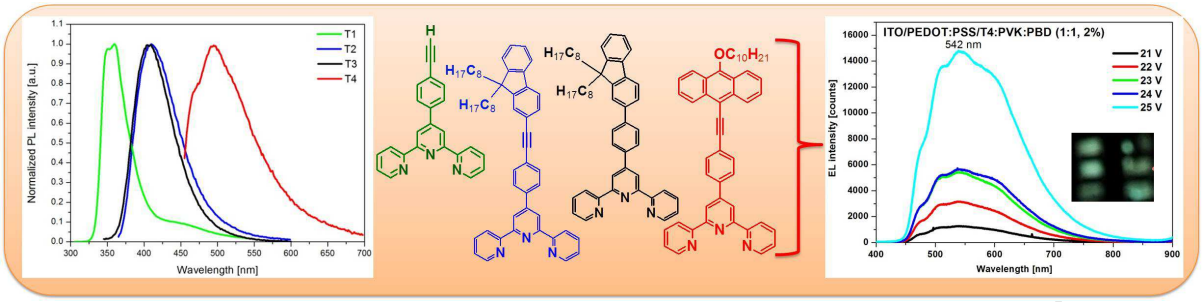

Highlights:

- Novel and well-soluble derivatives of 4'-phenyl-2,2':6',2''-terpyridine were obtained
- The influence of acetylene linker on thermal, electrochemical, optical and electroluminescence properties was examined
- Efficient luminophores with high photoluminescence (PL) and quantum yields (Φ)
- OLEDs devices containing **T1** and **T4** as emitters showed green to orange electroluminescence

Abstract

Novel derivatives of 4'-phenyl-2,2':6',2''-terpyridine (tpy) with ethynyl (**T1**), 2-ethynyl-9,9-dioctylfluorene (**T2**), 9,9-dioctylfluorene (**T3**), 9-ethynyl-10-decyloxyanthracene (**T4**) substituents were obtained via Sonogashira or Suzuki-Miyaura coupling reactions, respectively, and thoroughly characterized. The presence of ethynyl bridge impacts photophysical properties of novel compounds by shifting absorption and emission spectra towards longer wavelengths as compared to **T3**, where fluorene is connected with tpy via a single bond. TGA measurements showed that among the new terpyridines those obtained as solids exhibited high thermal stability as opposed to those which were oils (tpy containing fluorene motif). Due to the fact that high thermal stability of 4'-phenyl-2,2':6',2''-terpyridine derivatives showed photoluminescence (PL) quantum yield (Φ) in the range of 27 - 84% in solution, their electroluminescence ability was tested in diodes with guest-host configuration. For the ccompounds dispersed in a matrix consisting of poly(9-vinylcarbazole) (PVK) (50 wt %) and (2-*tert*-butylphenyl-5-biphenyl-1,3,4-oxadiazole) (PBD) (50 wt %) radiation with maxima between 374 to 531 nm and characterized with Φ in the range of 8 - 12% was observed. They exhibited green or violet electroluminescence. The results confirmed substantial role of aryl groups and the linker in the presented terpyridines in terms of their thermal, electrochemical, optical and electroluminescence properties. In addition, density functional theory (DFT) and time-dependent-density functional theory (TD-DFT) calculations were performed to provide an independent support and deeper insight into the experimental results.

Key words: Terpyridines, Organic electronics, Luminescence, DFT study, Fluorene, Anthracene

1. Introduction

For almost ninety years many derivatives of 2,2':6',2"-terpyridine (tpy) functionalized at different positions have been synthesised [1-3] and these efforts were mainly driven by their distinguished photophysical and electrochemical properties [4-6]. In particular, tpy derivatives due to their high binding affinity toward transition-metal (tridentate ligand feature), π-stacking ability, directed *H*-bond formation and synthetic accessibility have become frequently used units in material chemistry research related to organic electronics, medicine, catalysis and optoelectronics [6-11].

Simple 2,2':6',2"-terpyridine derivatives can be synthesised based on the Kröhnke reaction, which is a one-pot reaction using commercially available materials in simple medium [12, 13]. Products obtained in this way can be used in other reactions, i.e. coupling reaction, which allows to obtain materials with desired photophysical properties. Derivatives of 4'-phenyl-2,2':6',2"-terpyridine can be obtained in Suzuki-Miyaura cross-coupling reaction from appropriate precursors. 4'-(4-Ethynylphenyl)-2,2':6',2"-terpyridine and its derivatives can be synthesised in Sonogashira cross-coupling reaction [14, 15].

The differences between 4'-phenyl-2,2':6',2"-terpyridine and 4'-(4-ethynylphenyl)-2,2':6',2"-terpyridine with the same substituent was studied by Guowei Gao et al. based on corannulene motif [16]. They showed that compound with acetylene linker exhibits a bathochromic shift of absorption spectrum and higher fluorescence quantum yield in comparison to compound with substituent connected directly to phenyl. Furthermore, triple bond enhances the conjugation of the molecule and enables more efficient energy transfer.

In the literature there are described 4'-phenyl-2,2':6',2"-terpyridine derivatives with ethynyl [17-19], 9,9-dihexylfluorene, [15] and 2-ethynyl-9,9-dihexylfluorene [15, 20] substituents, but results are focused primarily on the synthesis of these compounds, while either photophysical or electrochemical properties as well as *in silico* investigations are rarely discussed. A series of bis(terpyridine) isomers referred to 2-TerPyB, 3-TerPyB, and 4-TerPyB was investigated and studied as electron-transport materials in OLEDs with extremely low operating voltage of 2.2 V at a luminance of 1 cd m^{-2} [21]. Terpyridine/diphenylamine derivatives used as blue fluorescent emitters and red phosphorescent hosts in OLEDs provided the maximum external quantum efficiency (EQE) of 4.9% in non-doped blue fluorescent OLEDs and as host materials in red phosphorescent OLEDs exhibited maximum EQE of 20.9% [22].

To the best of our knowledge, 4'-(4-ethynylphenyl)-2,2':6',2"-terpyridines with anthracene motif have not been described.

Herein, we described the synthesis of 4'-phenyl-2,2':6',2''-terpyridine with ethynyl (**T1**), 9,9-dioctylfluorene (**T2**), 2-ethynyl-9,9-dioctylfluorene (**T3**), 10-decyloxyanthracene (**T4**) substituents. The synthesis effort have been complemented by detailed spectroscopic, photophysical, theoretical and electrochemical studies with compounds **T1** and **T4** being tested in diodes with guest-host configuration.

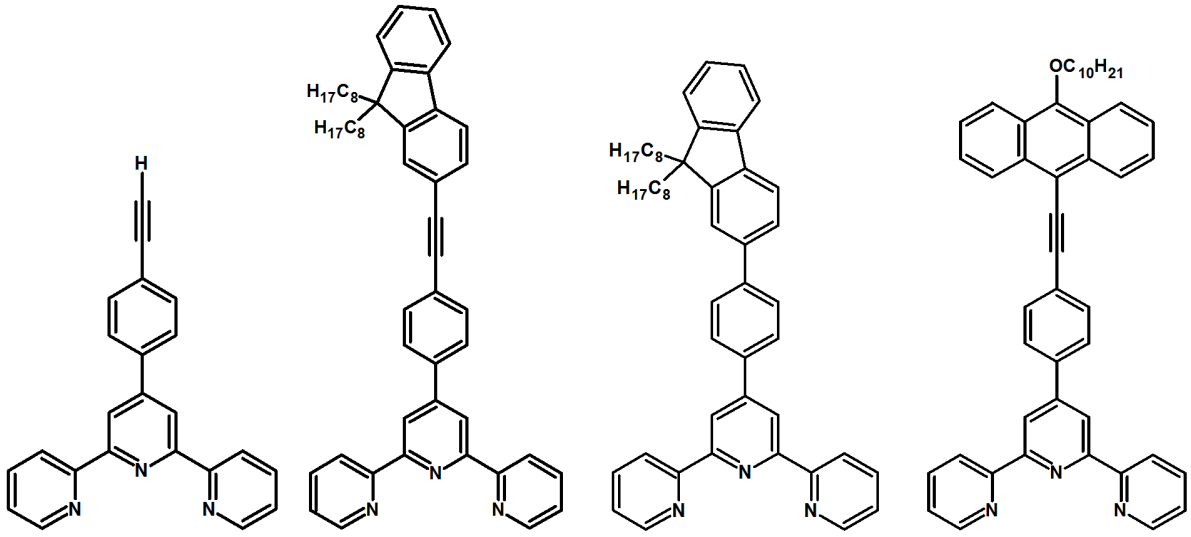

T1 **T2** **T3** **T4**

Figure 1. Structure of 4'-phenyl-2,2':6',2''-terpyridine derivatives **T1**-**T4**.

2. Results and discussion

2.1. Synthesis and structural characterization

The structure of designed 4'-phenyl-2,2':6',2''-terpyridine derivatives **T1-T4** is presented in Figure 1. Scheme 1 shows the synthesis route to 4'-(4-ethynylphenyl)-2,2':6',2''-terpyridine (**T1**) and intermediate 4′-(4-(4,4,5,5-tetramethyl-1,3,2-dioxaborolan-2-yl)phenyl)-2,2′,6′,2″-terpyridine (**2**). The first step was conducted based on the well-known procedures from commercially available 4-bromobenzaldehyde and 2-acetylpyridine in Kröhnke reaction, which resulted in 4'-(4-bromophenyl)-2,2':6',2''-terpyridine [23]. The Sonogashira cross-coupling reaction of **1** with trimethylsilylacetylene (TMSA) catalyzed by [$Pd(PPh_3)_4$] gave 4'-(4-ethynylphenyl)-2,2':6',2''-terpyridine (**T1**) with 92% yield [24]. Boronate ester **2** was obtained in the Suzuki-Miyaura coupling reaction between **1** and bis(pinacolato)diboron with

catalyst [Pd(pddf)$_2$Cl$_2$] with 33% yield [25, 26]. The routes of synthesis of aryl intermediates are presented in Scheme 2. Iodoarene **4** was obtained from commercially available fluorene upon iodination followed by alkylation under phase-transfer catalysis (PTC) conditions to afford 2-iodo-9,9-dioctylfluorene (**4**) with 79% yield [27, 28]. Intermediate **6** was obtained from commercially available anthrone in alkylation reaction followed by bromination resulting in 9-bromo-10-decyloxyanthracene with 26% yield.

The target 4'-(4-ethynylphenyl)-2,2':6',2''-terpyridine derivatives **T2** and **T4** were obtained in [Pd]/[Cu]-catalyzed Sonogashira cross-coupling reaction with respective haloaromatics **4** or **6** (Scheme 3). The desired 4'-phenyl-2,2':6',2''-terpyridine derivative **T3** was obtained in [Pd]-catalyzed Suzuki-Miyaura cross-coupling reaction with iodoarene **4**. The yields of conducted reactions were in the range of 26 - 92%. The compounds **T1** and **T4** were obtained as solids (**T1** - beige, **T4** - orange), compounds **T2** and **T3** were obtained as oils (**T2** - dark yellow, **T3** - yellow-orange).

The novel compounds **T1-T4** were fully characterized by standard spectroscopic methods ^{1}H and ^{13}C NMR and mass spectrometry. In addition, all the resulting compounds are perfectly soluble in organic solvents such as dichloromethane, chloroform, acetone, tetrahydrofuran, ethyl acetate, what allows to easy purification and characterization. Moreover, they are easy to handle, what is important for device preparation.

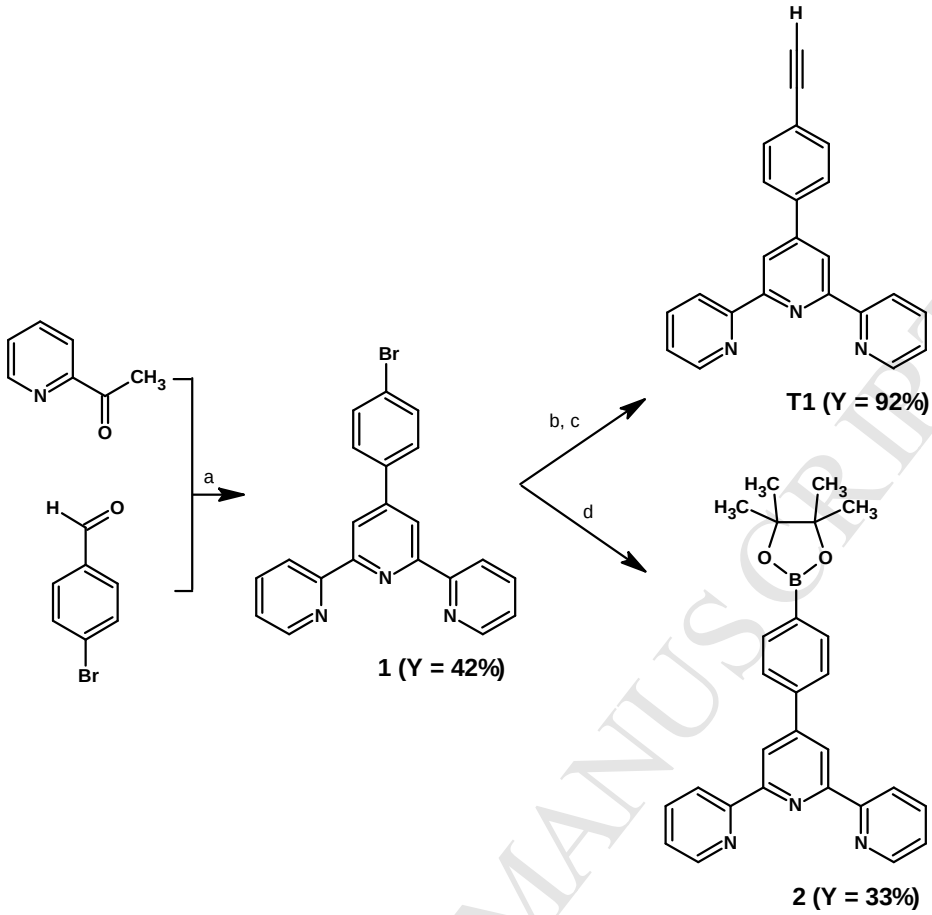

165

166 Scheme 1. Synthesis route of compounds **1**, **2**, and **T1**. *Reagents and conditions*: a) KOH,
167 $NH_{3\ aq}$, EtOH, room temp., 24 h; b) TMSA, $[Pd(PPh_3)_4]$, CuI, NEt_3, reflux, 16 h; c) KF, THF,
168 MeOH, room temp., 24 h; d) bis(pinacolato)diboron, $[PdCl_2(dppf)]$, KOAc, DMSO, 80 °C,
169 6 h.

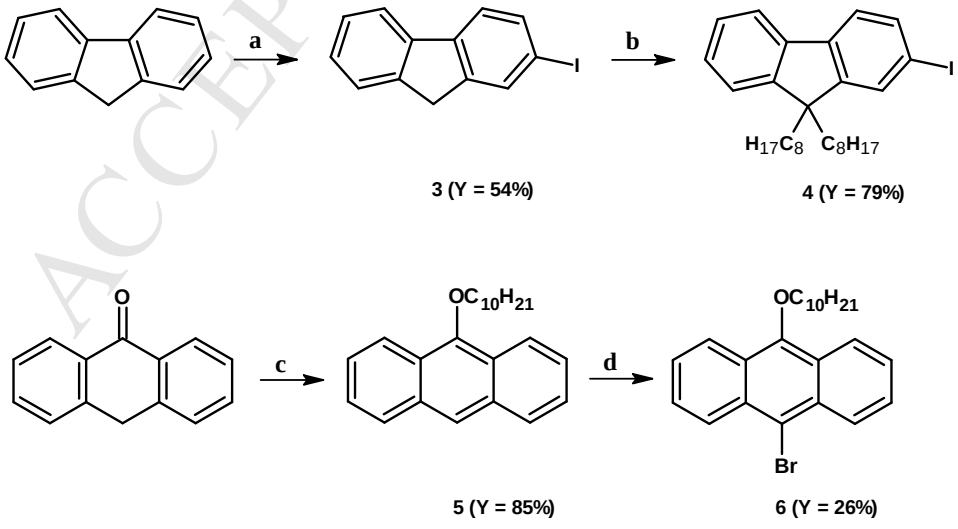

170

Scheme 2. Synthesis routes of compounds **3-6**. *Reagents and conditions*: a) I_2, H_5IO_6, $AcOH/H_2O/H_2SO_4$, 70 °C, 6 h; b) 50% $NaOH_{(aq)}$, TBAB, *n*-$C_8H_{17}Br$, DMSO, room temp., 12 h; c) *n*-$C_{10}H_{21}Br$; TBAI, KOH, H_2O, toluene, rf, 5 h; d) NBS, DMF, room temp., 12 h.

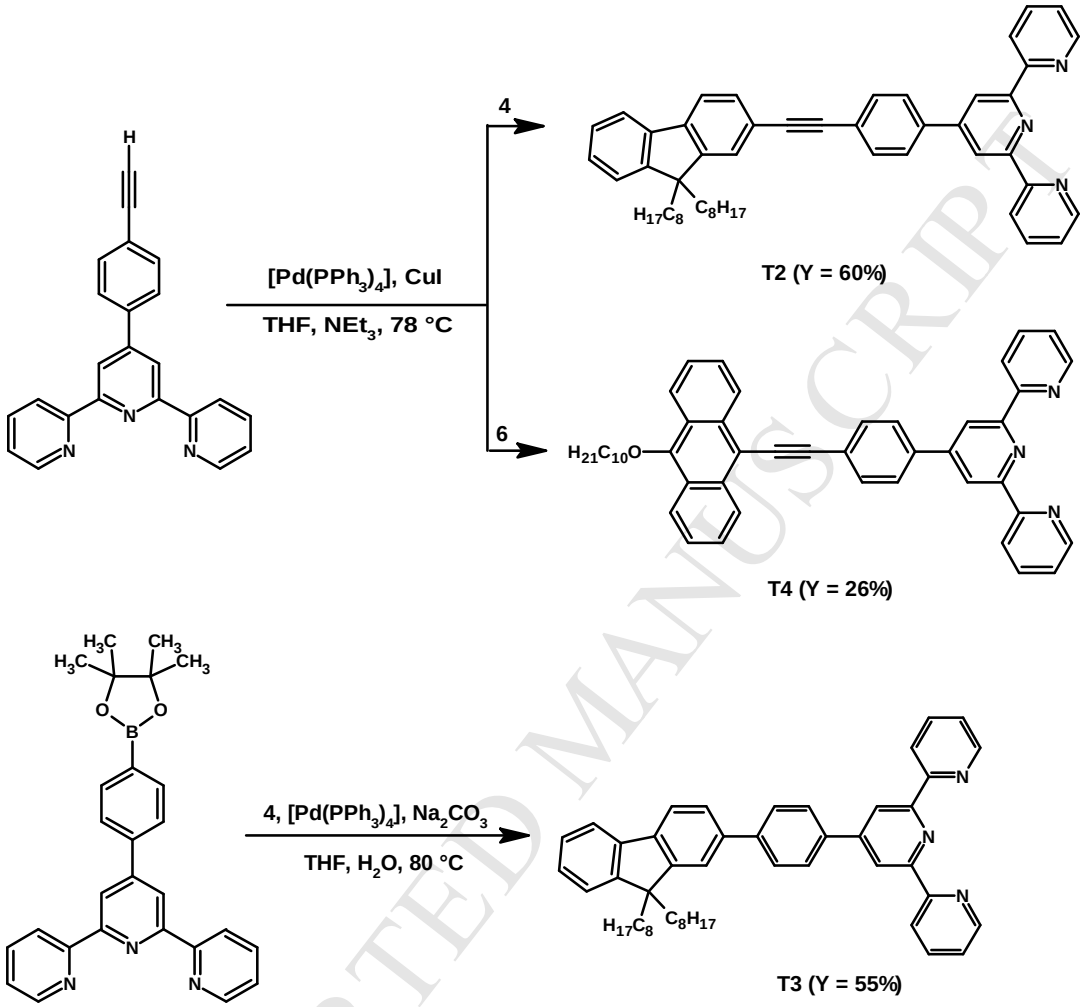

Scheme 3. Synthetic routes for the preparation of **T2-T4**.

2.2. Thermal properties

The thermal stability of the prepared 4'-phenyl-2,2':6',2''-terpyridine derivatives was evaluated using thermogravimetric analysis (TGA) under nitrogen atmosphere and the obtained data are presented in Table 1, whereas Figure 2 depicts representative TGA and DTG thermograms of compounds **T2** and **T4**.

Table 1. Thermal stability of **T1-T4** compounds.

Code	TGA		
	T_d [°C]	T_{max} [°C]	Char residue at 900 °C [%]
T1	309	307, 441, 565, 638, 734	61
T2	137	460	28
T3	145	468, 507	10
T4	286	348, 394	38

T_d – temperature of 5% weight loss, T_{max} – the maximum decomposition rate from DTG thermograms.

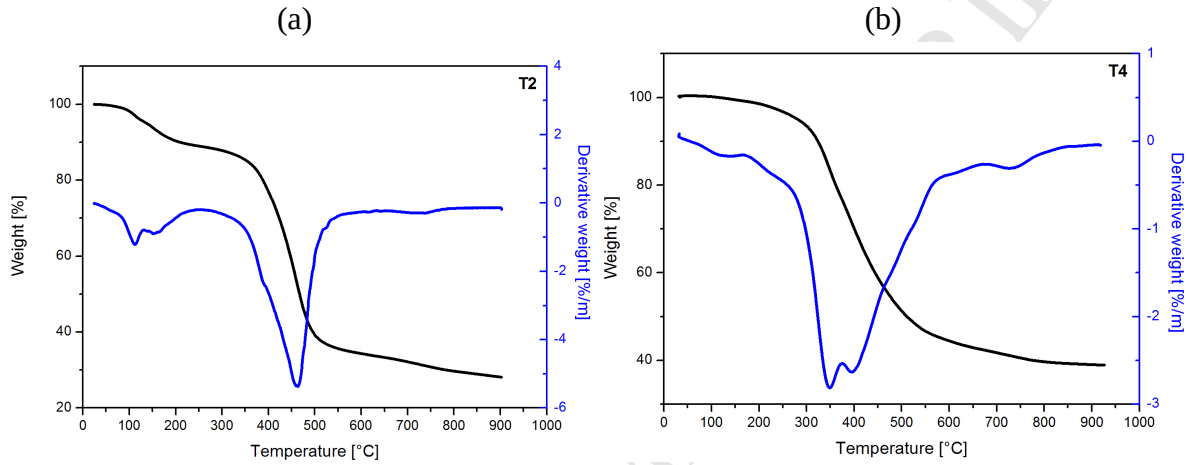

Figure 2. TGA with DTG curves of **T2** (a) and **T4** (b).

The TGA curves showed that the beginning of decomposition (T_d), which corresponds to the temperature of 5% sample weight loss during heating, was the highest for **T1** and **T4**. Introduction of fluorene unit to tpy frame (**T2** and **T3**) significantly lowered T_d. The presence of acetylene bond provided higher amount of the char residue. It was found that compound **T1** possessing only the ethylene substituent has better thermal stability than other compounds. DTG curves revealed that compounds with fluorene derivative exhibit one (for **T2**) and two (for **T3**) weight-loss peaks. The presence of acetylene linker has minimal impact on the thermal stability. In the case of **T4** the weight-loss peak with two maxima was registered. Additionally, for compounds which were in a solid state, that is **T1** and **T4**, the differential scanning calorimetry (DSC) measurements were carried out. The first heating scan of **T1** revealed two endotherms with maximum at 129 and 175 °C. DSC thermogram registered at second heating run after rapid cooling showed only glass transition temperature (T_g) at 62 °C. During further heating of **T1** above 175 °C at first heating run the exotherme was seen with a maximum at 198 °C. 4'-Phenyl-2,2':6',2''-terpyridine derivative denoted as **T4** was also molecular glass with T_g at 33 °C obtained in second heating DSC scan. Further

heating above T_g revealed crystallization and melting peaks at 143 and 157 °C, respectively. The first heating of **T4** yields crystallization and melting peaks at 87 and 156 °C, typical of a monophase crystalline solid.

2.3. DFT studies

To gain useful information about the geometry and optical properties of obtained terpyridines **T1**-**T4** the density functional theory (DFT) and time-dependent-density functional theory (TD-DFT) calculations were performed. The B3LYP exchange-correlation functional with 6-31G** basis set, as implemented in the Gaussian 09 program, was employed [29]. The B3LYP/6-31G** geometries were optimized in dichloromethane solution in the polarisable continuous model (PCM), structures for **T1**-**T4** are presented in Table 2. It can be seen that the connecting phenyl ring and the central pyridine ring are twisted by about 35º with respect to each other. The substituents connected via triple bond in **T2** and **T4** are in coplanar position to phenyl ring, while in **T3** the fluorene motif is twisted by about 35º. One can see that acetylene linkage improves the planarity of the substituents. The geometry affects the photophysical properties, for instance, the **T2** compound due to its coplanarity shows higher quantum yield in comparison to the compound with substituent connected direct to phenyl **T3**. The triple bond causes the faster and more efficient energy transfer.

Electrostatic potential energy maps for **T1**-**T4** are showed in Figure S10 (Supporting Information), they illustrate three-dimensional charge distributions of molecules. It determines mutual interactions between molecules, but also – which is important in our case - it confirms the tridentate ligands feature.

A schematic representation of the frontier molecular orbitals and the energy gaps (ΔE) between the highest occupied molecular orbital (HOMO) and the lowest unoccupied molecular orbital (LUMO) for described compounds is presented in Figure 3. The value of ΔE for **T1**-**T4** is respectively 4.60, 3.63, 3.98, and 2.79 eV.

In the case of **T2** and **T4** the electrons in the HOMO are mainly localized on the aryl substituents, ethynyl linkage, and terminal phenyl ring. The HOMO of **T3** is located on the aryl motif and terminal ring. The LUMOs of **T2** and **T4** are mainly delocalized on ethynyl bridge, phenyl ring and, partially, on central pyridine ring and aryl motif. Localization of LUMO in **T3** is similar, but due to the absence of triple bond, a larger part of LUMO is delocalized on terpyridine unit. Moreover, the alkyl chains participate neither in HOMO nor in LUMO energy levels, thus giving little influence on the optical properties, but on the other

hand, their existence significantly improves the solubility of compounds. The introduction of acetylene linker to **T3** has no effect on the localization of frontier molecular orbitals. Occupied frontier orbital for **T1** is also localized on ethynyl linkage, and terminal phenyl ring, but the HOMO is delocalized on almost the whole molecule.

The next part of *in silico* studies concerns prediction of absorption spectra by using TD-DFT calculations, which were also carried out at the B3LYP level of theory with a 6-31G** basis set. Calculated wavelengths in absorption spectra, oscillator frequencies (f) and transitions for the highest oscillators (f > 0.20) are listed in Table 3. The obtained results compared to experimental data show shifts. In the range of calculated absorption spectra five (**T1**), six (**T2**, **T3**) and twelve (**T4**) main bands were seen. What is more, the experimental absorption bands are wide, what can cause diminishing of other, less intense bands. The differences of the absorption energies of examined compounds **T1**-**T4** with experimental data may be related to solvent polarity and explained by specific solvent effects.

Table 2. B3LYP/6-31G** calculated geometries for **T1**-**T4**.

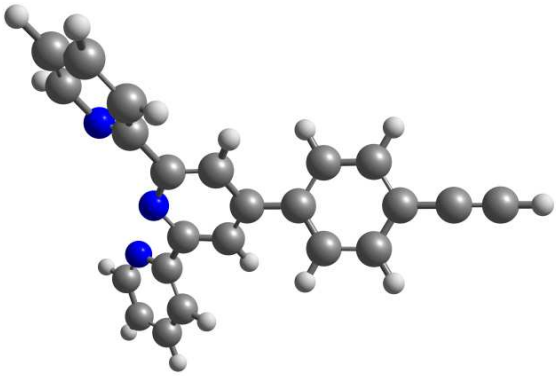

T1

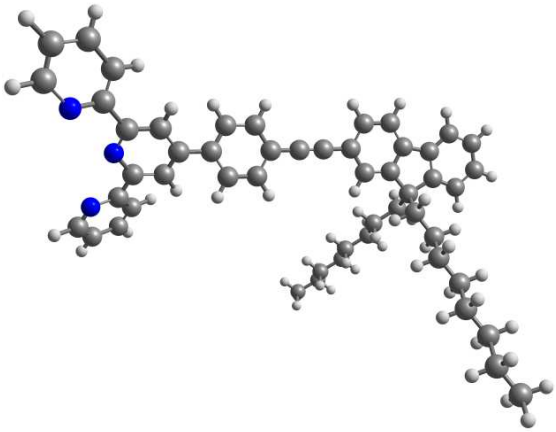

T2

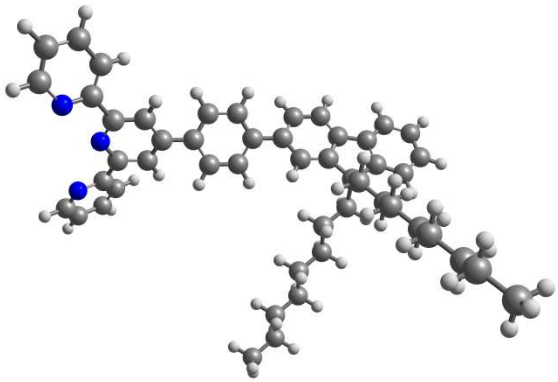

T3

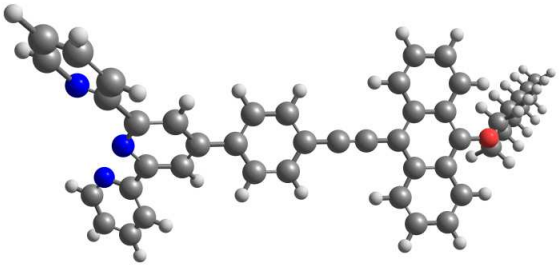

T4

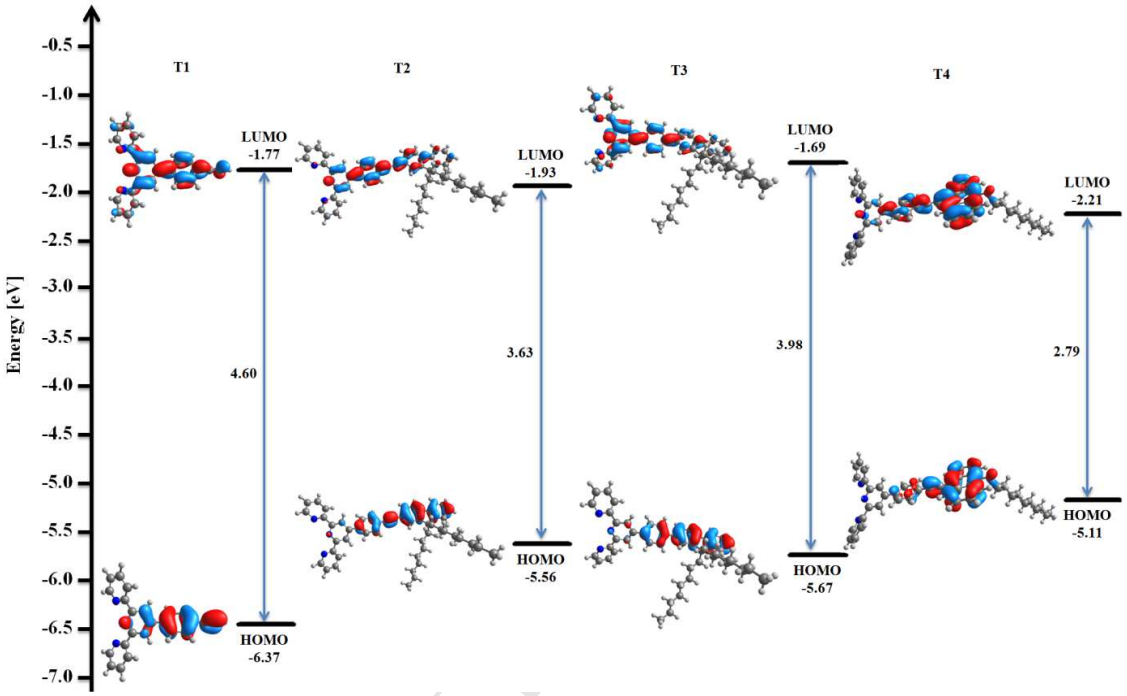

Figure 3. Schematic representation of the molecular orbitals for **T1-T4**.

Table 3. Wavelength maxima [nm] of absorption spectra together with oscillator strengths calculated for **T1-T4** molecules with TD-DFT method.

Code	Calculated wavelengths [nm] (oscillator strengths)	Transitions
T1	302 (0.17)	
	295 (0.58)	H-2→LUMO (25%), HOMO→LUMO (62%), H-1→LUMO (4%)
	294 (0.29)	H-2→LUMO (53%), HOMO→LUMO (30%), H-6→LUMO (3%), H-5→LUMO (5%), H-2→L+2 (3%)
	264 (0.27)	H-1→L+1 (86%), H-3→L+1 (3%), HOMO→L+2 (4%)
	250 (0.24)	H-1→L+2 (78%), H-4→L+1 (8%), H-1→L+4 (3%)
T2	384 (1.86)	HOMO→LUMO (98%)
	314 (0.26)	HOMO→L+2 (95%), H-2→LUMO (2%)
	303 (0.15)	

	291 (0.10)	
	263 (0.13)	
	258 (0.18)	
T3	347 (1.16)	HOMO→LUMO (97%)
	295 (0.40)	HOMO→L+2 (87%), H-1→LUMO (6%)
	294 (0.22)	H-1→LUMO (74%), H-2→L+1 (2%), H-1→L+2 (2%), HOMO→L+1 (8%), HOMO→L+2 (7%)
	270 (0.11)	
	263 (0.19)	
	253 (0.18)	
T4	480 (0.89)	HOMO→LUMO (99%)
	332 (0.24)	H-1→LUMO (85%), H-2→LUMO (2%), HOMO→L+1 (2%), HOMO→L+3 (7%)
	318 (0.29)	HOMO→L+3 (86%), H-1→LUMO (8%)
	278 (0.14)	
	277 (0.16)	
	276 (0.27)	H-10→LUMO (20%), H-3→LUMO (20%), HOMO→L+6 (14%), HOMO→L+8 (18%) H-11→LUMO (4%), H-7→LUMO (2%), H-5→L+2 (2%), H-3→L+1 (6%)
	273 (0.12)	
	272 (0.15)	
	267 (0.16)	
	263 (0.22)	H-2→L+2 (84%)
	254 (0.47)	H-3→L+1 (78%), HOMO→L+6 (11%), H-1→L+6 (5%)
	247 (0.18)	

2.4. Photophysical properties

2.4.1. UV-Vis absorption and photoluminescence in solution

The UV-Vis absorption and photoluminescence emission (PL) spectra of the terpyridine derivatives **T1**-**T4** were investigated in dichloromethane (CH_2Cl_2) solution at room temperature and are presented in Figure 4a and b. The terpyridines **T1**-**T4** exhibit broad absorption spectra between 239 and 449 nm. The absorption set of each compound consists at least of three peaks. The first absorption bands for **T1**-**T4** are located between 239 and 324 nm and can be identified with $\pi \rightarrow \pi^*$ transitions of the conjugated pyridine rings [30]. For compounds **T2**-**T4** the additional absorption bands appear between 340 and 449 nm, which can be ascribed to the intramolecular charge transfer (ICT) states between fluorene and anthracene units acting as donors and electron-accepting terpyridines. The absorption bands of **T4** are considerably red-shifted compared to **T2** and **T3**, indicating stronger ICT

interaction in **T4** caused by higher donor ability of 9-decyloxyanthracene substituent. Moreover, the maximum absorption peaks of **T3**, with a single bond, is shifted to shorter wavelengths by around 19 nm as compared to compound **T2** with acetylene linkage between tpy and fluorene units. The observed red-shift with respect to **T3** is attributed to extension of π conjugation.

Photoluminescence properties of compounds **T1**-**T4** recorded in CH_2Cl_2 solutions are presented in Figure 4b and the obtained data are collected in Table 4. The PL spectra of **T1**-**T4** in solution feature strong emission peaks in the range of 349-495 nm. The maxima of emission decrease from **T1** (359 nm) through **T3** (407 nm) and **T2** (410 nm) to **T4** (495 nm), which is related to the structure of the investigated terpyridine derivatives. The compound **T1** emits blue light, whereas the presence of additional terminal substituents, such as fluorene (**T2** and **T3**) and anthracene (**T4**) in the backbone, generates the blue-reddish (**T2** and **T3**) and orange (**T4**) emission. The emission maximum of compound **T3** possessing fluorene connected with tpy backbone via single bond, is centered at 407 nm, which is shifted by about 3 nm towards shorter wavelengths with respect to that of **T2**, which is modified by extended spacer. Furthermore, the introduction of the pendant 9-decyloxyanthracene fragment in **T4** generates a considerable red-shift of emission maximum, as compared to the other three compounds (**T1**-**T3)**. This points out at the strongest electron-donating capacity of anthracene unit, and thus the resulting highly conjugated π-electron structure of **T4**. The quantum yields of **T1**-**T4** emission are in the range from 27 to 84%. The addition of terminal substituents into phenyl-terpyridine backbone significantly increases the quantum yields from 27% for **T1** ended by ethynyl chain to 84% for **T2**, which possesses 9,9-dioctylfluorene and ethylene linkage. In addition, in the case of **T2** and **T3**, the difference only in the character of spacer yields to large (>20%) change in quantum efficiencies. Comparing the value of quantum yield of **T3** (Φ_f=0.62) and **T2** (Φ_f=0.84) varying only by ethylene linker, to that of the described 4'-(4-(9,9-dihexyl-9H-fluoren-2-yl)phenyl)-2,2':6',2″-terpyridine (Φ_f=0.92) [31], the Φ value of the former is higher than that of **T3** and comparable to **T2**. This implies that the presence of additional linker connecting the peripheral substituents to terpyridine moiety contribute to the enhancement of Φ value. Furthermore, the obtained Φ values for **T1**-**T4** are considerably higher than that observed for symmetrically substituted bis(terpyridines) with different aromatic spacer (Φ_f=0.20-0.58) [32]. The measured lifetime (τ) values for **T1**-**T4** range from 1.02 to 2.97 ns. Among the studied compounds, compound **T1** exhibits the longest fluorescence lifetime (τ=2.97 ns) resulted from the most planar geometry. Meanwhile, the rigid connection of fluorene unit

with terpyridine backbone in **T3** gives rise to longer lifetime (τ=1.24 ns) than the flexible ethylene spacer in **T2** (τ=1.02 ns).

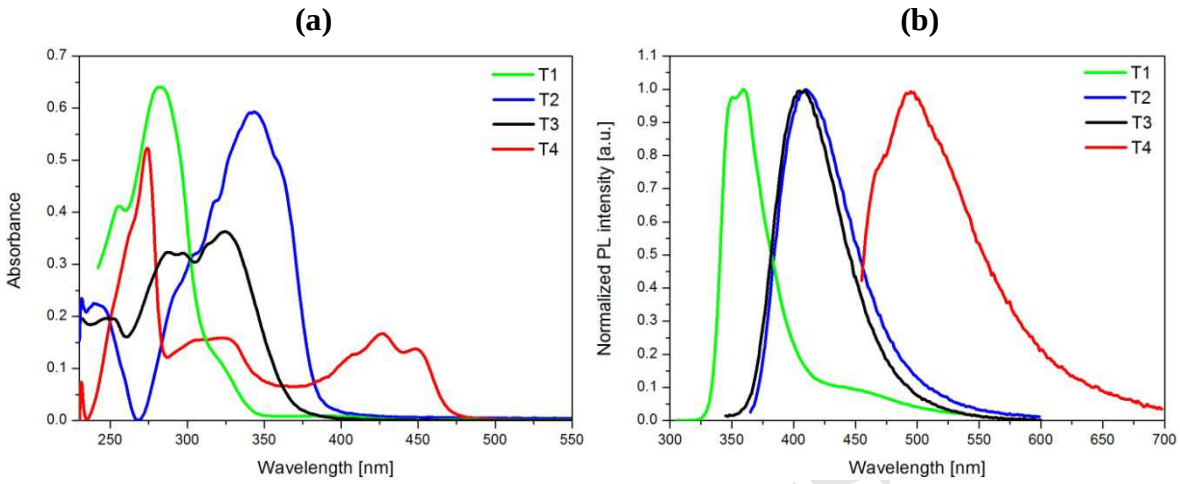

Figure 4. (a) The UV-Vis and (b) PL spectra of **T1**-**T4** in dichloromethane solution (c = 10^{-5} mol/L).

Table 4. UV-Vis, PL, quantum yield and lifetime data of **T1**-**T4** compounds dissolved in dichloromethane (c=10^{-5} mol/L).

Code	**λ_{max} [nm] ($\varepsilon/10^{-5}$ M^{-1} cm^{-1})**	**PL λ_{ex} [nm]**	**PL λ_{em} [nm]/ Stokes shift [cm^{-1}]**	**Φ [%]**	**τ [ns]**
T1	256 (0.41), 283 (0.64)	320	349/6682; 359/7480	27	2.93
T2	239 (0.23), 343 (0.59)	338	410/4764	84	1.02
T3	248 (0.20), 288 (0.32), 297 (0.32), 324 (0.36)	327	407/6294	62	1.24
T4	274 (0.53), 325 (0.16), 427 (0.17), 449 (0.14)	421	495/3217	55	2.73

The results of optical spectroscopy studies in solution show that the character of substituents and spacer has prominent influence on the photophysical properties of the terpyridine derivatives **T1**-**T4**. Summarizing, the tpy derivatives are promising luminescent materials with relatively high quantum yields, broad absorption spectra and enhanced ICT interactions, when the electron-donating units and highly π-electron spacers are introduced into the terpyridine molecule.

2.4.2. UV-Vis photoluminescence and electroluminescence in solid state

The investigations of ability to photo- and electroluminescence (EL) in solid state as film and in a matrix consisting of poly(9-vinylcarbazole) (PVK) (50 wt %) and (2-tert-butylphenyl-5-

biphenyl-1,3,4-oxadiazole) (PBD) (50 wt %) were performed for **T1** and **T4** compounds. Their good thermal stability, solubility and solid state character with high PL quantum field in solution suggested that they can be considered as promising candidates for OLEDs. Additionally, UV-Vis spectra of **T1** and **T4** as thin films on glass substrate were registered. As compared to absorption spectra obtained in solution, bathochromic shift of λ_{max} by about 27 and 4 nm for **T1** and **T4** in films was seen, respectively (Figure 5a). Photoluminescence data are gathered in Table 5, whereas the representative PL spectra are depicted in Figure 5.

Table 5. Photoluminescence data of **T1** and **T4** layers.

Code	Medium	PL λ_{ex} [nm]	PL λ_{em} [nm]	Φ [%]
T1	Film	310	**378**, **510**^{sh}	8.02
		340	374, 510^{sh}	-
	Blend PVK:PBD[a]	310	**410**	10.60
		340	410	-
		350	410	-
T4	Film	310	377, 467, 531	1.75, -, 1.81
		340	414, 513	-
		350	414, 437, 520	-
		380	**439**, 522^{sh}	2.05
	Blend PVK:PBD[a]	310	404, **464**	11.41, 8.74
		340	404, 464	-
		350	411	-

[a] 2 wt % content of compound in PVK:PBD (50:50 in weight %). – not measured. Bold data indicated the most intense luminescence.

PL spectra were registered for various excitation wavelength (λ_{ex}). The most intense emission was observed under λ_{ex} equal to 310 nm, except for **T4** in film. Contrary to **T4**, in the case of **T1** as film one emission band with a shoulder was seen. In the PL spectra of **T4** two main emission bands are observed, which changed their respective intensities with decrease of λ_{ex} energy and finally under λ_{ex} =380 nm band with λ_{em} at 439 and with shoulder at 522 nm was seen (Figure 5b). The maximum emission band in film and blend of **T1** was bathochromically shifted compared to solution and the opposite behaviour was registered for **T4** (Table 4 and Table 5). The higher PL quantum yield (Φ) was found for **T1**. In both cases the PL Φ were higher for blends than for films.

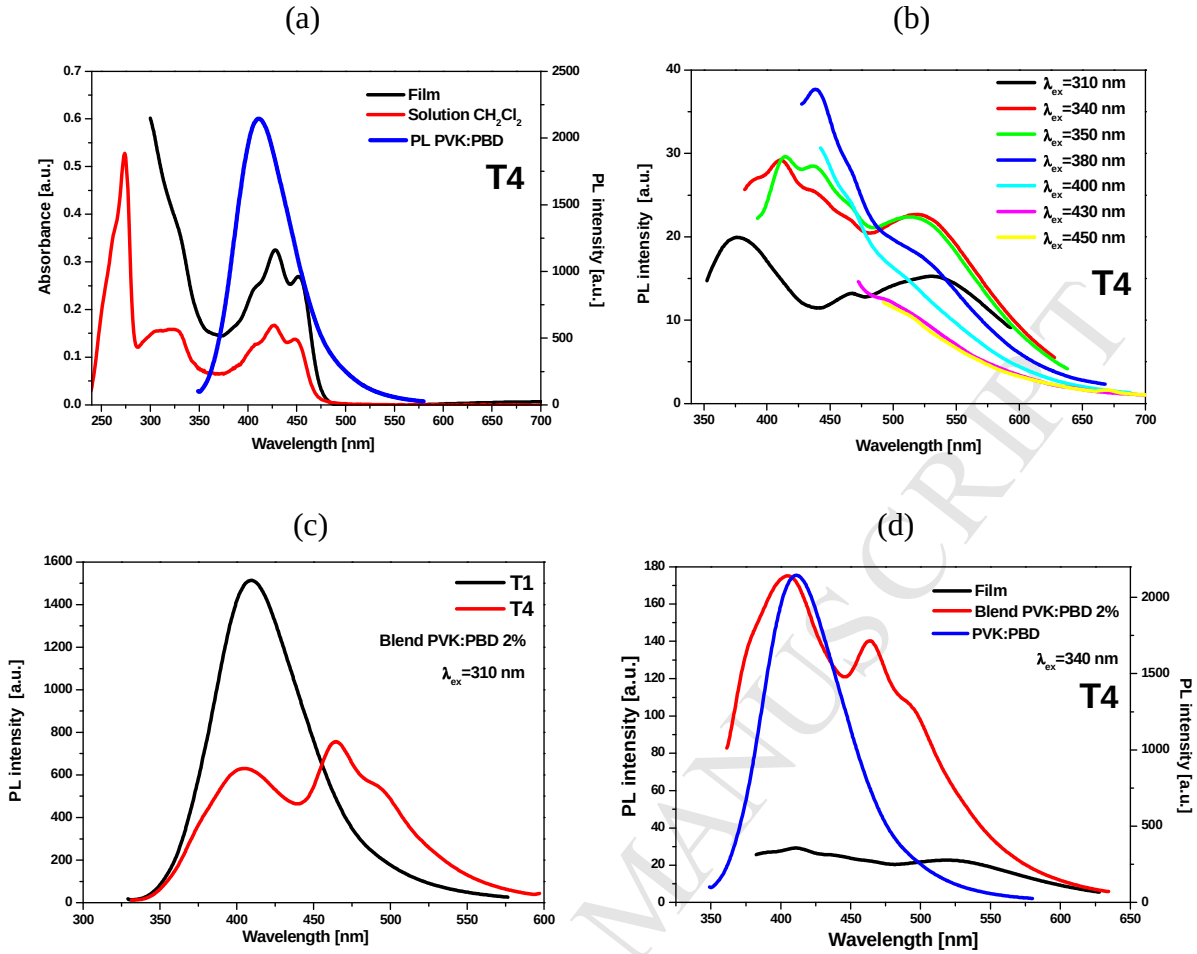

Figure 5. (a) UV-Vis spectra of **T4** with PL spectrum of matrix, (b) PL spectra of **T4** as film under various excitations wavelength, (c) PL spectra of **T1** and **T4** under λ_{ex} =310 nm, and (d) PL spectra of **T4** in film and blend under λ_{ex} =340 nm.

Considering UV-Vis spectra of **T4** film and PL spectra of matrix in the guest - host diode configuration, Förster energy transfer from host (PVK:PBD) to guest can be expected (Figure 5a). In PL spectrum of **T4** dispersed molecularly in PVK:PBD under λ_{ex} =340 nm, which is the best for excitation of binary matrix, two emission bands were found with λ_{em} hypsochromically shifted as compared to film. The PL band with λ_{em} at 404 nm of blend may overlap with the emission band of matrix, thus, it is difficult to conclusively comment on the completeness of the energy transfer.

In the next step, electroluminescence ability of **T1** and **T4** was tested in diode with configuration: ITO/PEDOT:PSS/PVK:PBD:compound/Al. The current density-voltage (J-V) characteristics were registered up to 5 V (Figure 6).

(a)

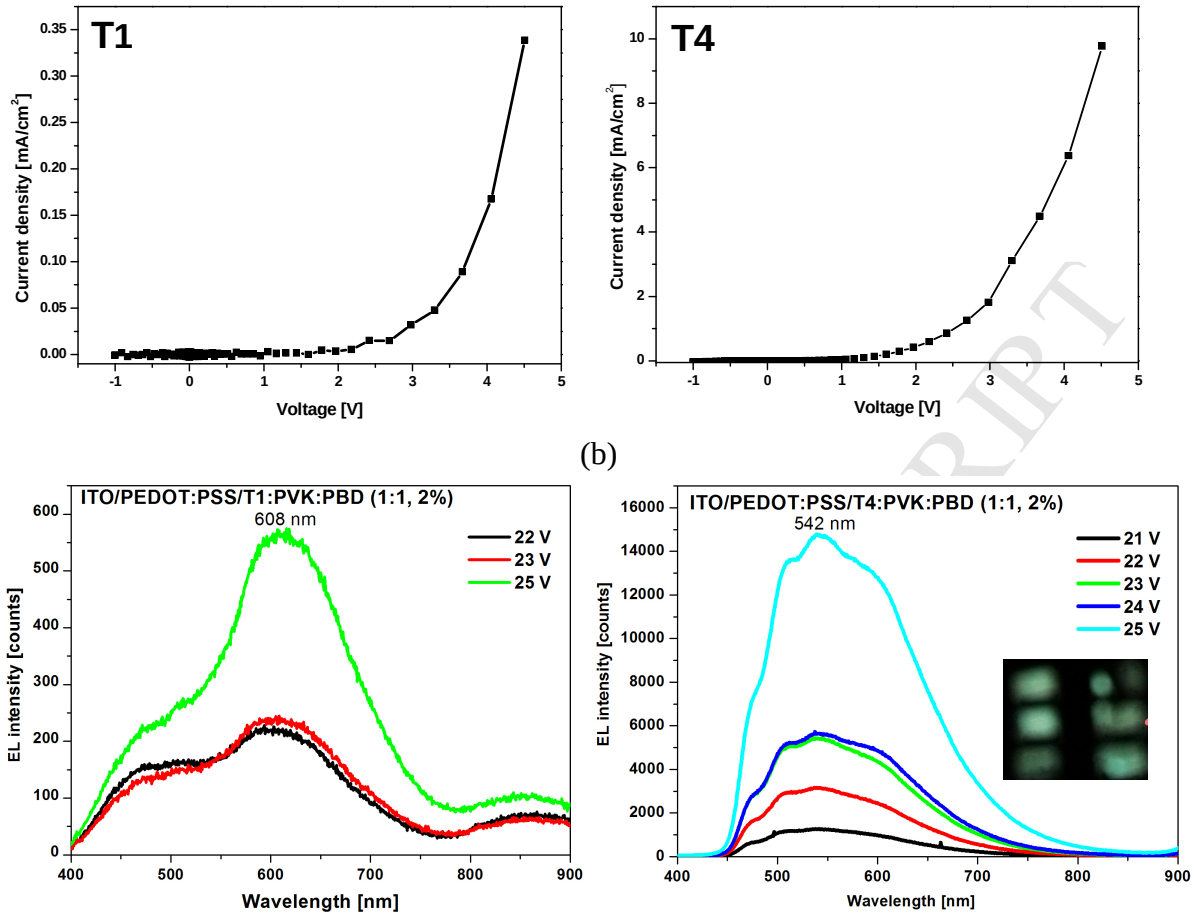

Figure 6. (a) Current density – voltage characteristic of devices based on **T1** and **T4** and (b) EL spectra of investigated compounds for increasing external voltage together with photo of diode based on **T4** under applied voltage.

The diodes showed low value of turn-on voltage (V_{on}), that is, 1.4 and 2.5 eV for devices based on **T1** and **T4**, respectively. It is worth noting that the OLED device based on terpyridine-substituted triphenylamine with rigid benzyl unit exhibited the turn-on voltage at 6.0 V with blue EL at 460 nm [33]. Both diodes with chromospheres **T1** and **T4** emitted light under applied voltage and their EL spectra are depicted in Figure 6. The diodes differ in both intensity of EL and the position of maximum of emission band (λ_{em}). Devices based on **T1** and **T4** emitted light from the orange and green spectral region, respectively. The significantly more intense EL was measured for the diode based on **T4**.

2.5. Electrochemical properties

The electrochemical properties of **T1**-**T4** were investigated in CH_2Cl_2 solution by means of cyclic voltammetry (CV) and differential pulse voltammetry (DPV). The representative

cyclic voltammograms are presented in Figure 7 (reduction) and Figure 8 (oxidation). DPV is depicted in Figure 9. The electrochemical oxidation and reduction onset potentials were used for estimation of the HOMO and LUMO energies (or rather, ionization potentials and electron affinities) of the materials (assuming that IP of ferrocene equals to 5.1 eV) [34]. The calculated HOMO and LUMO levels together with electrochemical energy band gap (E_g) are presented in Table 6.

For deeper understanding of the photophysical properties of investigated compounds a series of electrochemical measurements was carried out. The electrochemical properties of **T1**-**T4** were investigated in CH_2Cl_2 solution using glassy carbon (GC) as working electrode. First, the electrochemical properties during reduction process were investigated (Figure 7). All of the tested compounds undergo reduction between -2.07 (**T4**), and -2.30 V (**T3**) (so, at very similar potentials). Moreover, trends in LUMO energy are consistent in tendency with the values obtained by DFT calculations. On the other hand, differences observed during the oxidation process are more significant. The value of onsets of the first oxidation step for **T2** and **T3** is approximately equal. Thus, incorporation of acetylene linker into molecule does not affect this parameter. However, the type of this process is slightly different. As can be seen in Figure 8, for **T2** oxidation is irreversible, while in the case of **T3** it is rather reversible. Additionally, we have observed strong influence of electrode materials on determined values. As can be seen in Figure 8 (brown line) when measurement is carried out using gold electrode, oxidation take place at significantly lower potential (0.68 compared to 1.04 V in the case of GC electrode). In our opinion it is the consequence of strong interaction between terpyridine and the metallic surface, yielding species similar to gold complex. Determined value of E_{ox} is the lowest for **T4** (0.45 V), what can be attributed to strong electron donating character of alkoxy group. The electrochemically determined band gaps for all tested compounds differ significantly depending on the substituent. Also, as can be seen in Table 6, in each case above mentioned values agree well with calculated from UV-Vis spectroscopy.

Table 6. Electrochemical data for **T1**-**T4**.

	$E_{ox(CV)}$	$E_{ox(DPV)}$	$E_{red(CV)}$	$E_{red(DPV)}$	**HOMO [eV][1]**	**LUMO [eV][2]**	$E_{g\ el}$ **[eV][3]**	$E_{g\ opt}$ **[eV][4]**	$E_{g\ (DFT)}$ **[eV]**
T1	1.49	1.45	-2.22	-2.18	-6.59	-2.88	3.71	3.87	4.60
T2	1.04	1.02	-2.15	-2.12	-6.14	-2.95	3.19	3.18	3.63
T3	0.99	0.93	-2.30	-2.24	-6.09	-2.80	3.29	3.10	3.98

T4	0.45	0.33	-2.07	-2.06	-5.55	-3.03	2.52	2.64	2.79

[1]E_{HOMO}= - 5.1 - $E_{ox,\ onset}$; [2] E_{LUMO}= - 5.1 - $E_{red,\ onset}$; [3]$E_{g\ el}$ = $E_{ox,\ onset}$ - $E_{red,\ onset}$ = E_{HOMO} - E_{LUMO}

[4]calc. from: Eg=1240/λ_{abs}

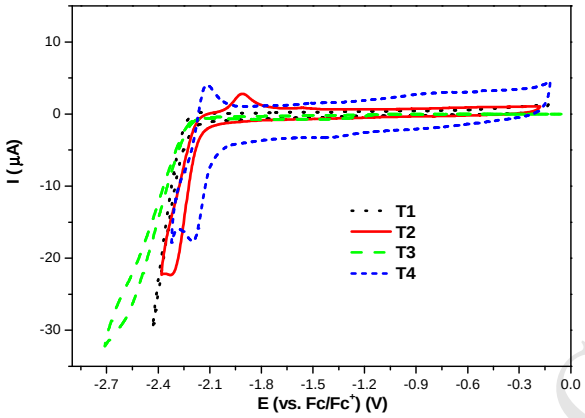

Figure 7. Cyclic voltammograms of **T1**-**T4** during oxidation; GC as working electrode; sweep rate ν = 100 mV/s, 0.1 M Bu_4NPF_6 in CH_2Cl_2. Peak onset potentials were used for estimation of the LUMO energies.

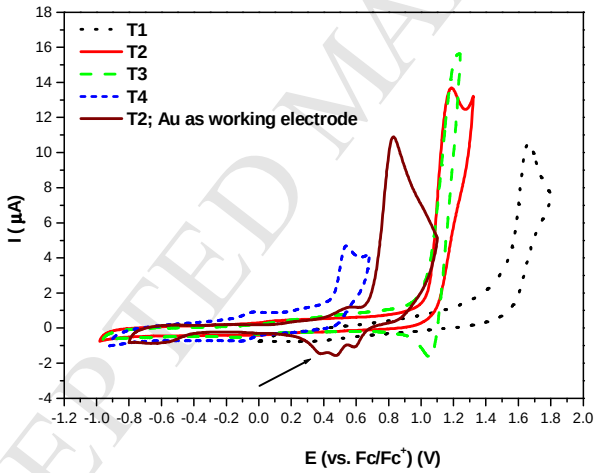

Figure 8. Cyclic voltammograms of **T1**-**T4** during oxidation; GC as working electrode (unless otherwise stated) ; sweep rate ν = 100 mV/s, 0.1 M Bu_4NPF_6 in CH_2Cl_2. Arrow indicates additionals peaks while measurment is carried out using gold electrode. Peak onset potentials were used for estimation of the HOMO energies.

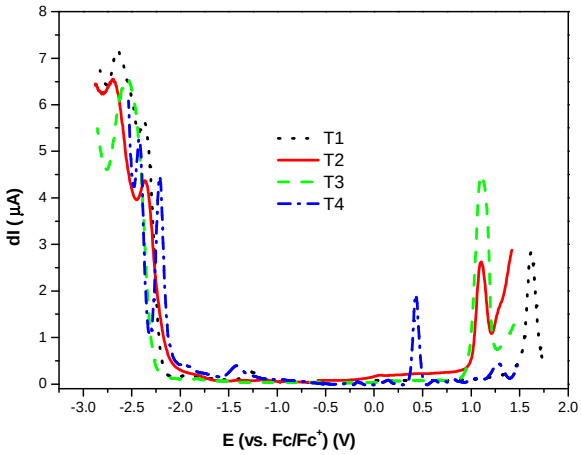

Figure 9. Differential pulse voltammograms of **T1**-**T4**; GC as working electrode; potential step = 2.5 mV/s, 0.1 M Bu_4NPF_6 in CH_2Cl_2.

3. Experimental Section

Materials

All chemicals and starting materials were commercially available and were used without further purification. Solvents were distilled as per the standard methods and purged with nitrogen before use. All reactions were carried out under argon atmosphere unless otherwise indicated. Column chromatography was carried out on Merck silica gel. Thin layer chromatography (TLC) was performed on silica gel (MerckTLCSilicaGel60).

4'-(4-Bromophenyl)-2,2':6',2"-terpyridine [24], 4′-(4-(4,4,5,5-tetramethyl-1,3,2-dioxaborolan-2-yl)phenyl)-2,2′,6′,2″-terpyridine [25, 26], 2-iodofluorene [27], 2-iodo-9,9-dioctylfluorene [28] were synthesized according to the reported procedures with minor modifications; 9-decyloxyanthracene, 9-bromo-10-decyloxyanthracene were obtained in innovative way. All compounds were characterized by ^1H NMR spectroscopic analysis (see the Supporting Information for details).

Procedure for the synthesis of 4′-(4-ethynylphenyl)-2,2′:6′,2′′-terpyridine T1

4'-(4-Bromophenyl)-2,2':6',2"-terpyridine (5.15 mmol, 2 g) and 140 mL of triethylamine were placed in two-neck round-bottom flask and bubbled with argon for 15 minutes. After this time $[Pd(PPh_3)_4]$ (0.52 mmol, 0.60 g), CuI (0.52 mmol, 0.10 g) were added. The resulting solution was stirred and then TMSA (10.3 mmol, 1.46 g) was added by using a syringe. Mixture was heated at 92 °C for 16 hours. The solution was evaporated and purified by

chromatography by using CH_2Cl_2 and EtOAc (20:1) as eluent resulting in white crystals. Obtained intermediate was dissolved in 50 mL of MeOH and 80 mL THF and bubbled with argon. Potassium fluoride (4.34 mmol, 0.25 g) was added and mixture was stirred at room temperature for 24 hours. The solution was evaporated and the residue was dissolved in 50 mL of CH_2Cl_2 and extracted with water (3 x 25 mL). The combined organic layers were dried under anhydrous $MgSO_4$ and filtered. After removing the solvent under reduced pressure the crude product was purified by chromatography by using CH_2Cl_2 and EtOAc (20:1) as eluent.

General Procedure for the synthesis of 4'-(4-ethynylphenyl)-2,2':6',2"-terpyridine derivatives in Sonogashira Cross-Coupling reaction for T2 and T4: 4'-(4-Ethynylphenyl)-2,2':6',2"-terpyridine (1.0 mmol, 0.33 g), $Pd(PPh_3)_4$ (0.06 mmol, 0.070 g) and CuI (0.06 mmol, 0.01 g) were placed in a 150 mL dry Schlenk flask. Then the flask was evacuated to vacuum and filled with argon for three times. Appropriate heteroaryl halide (1.2 mmol) was dissolved in 50 mL solution of THF and NEt_3 (1:1) and under inert atmosphere added to reaction flask. The resulting mixture was stirred at 78 °C for 48 hours. After the reaction was completed, the mixture was cooled down to room temperature and the solvents were evaporated under reduced pressure. The residue was dissolved in CH_2Cl_2 and extracted with water and brine and dried over anhydrous $MgSO_4$. The solvent was evaporated under reduced pressure, and the crude product was purified on column chromatography on silica gel, eluent: CH_2Cl_2 : EtOAc (20:1).

Procedure for the synthesis of 4'-(4-phenyl)-2,2':6',2"-terpyridine derivative in Suzuki - Miyaura Cross-Coupling reaction for T3: 4′-(4-(4,4,5,5-Tetramethyl-1,3,2-dioxaborolan-2-yl)phenyl)-2,2′,6′,2″-terpyridine (0.82 mmol, 0.36 g), 2-iodo-9,9-dioctyl-9H-fluorene (0.69 mmol, 0.35 g), 15 mL THF and solution of Na_2CO_3 (2.87 mmol, 0.30 g in 3 mL H_2O) were placed in a 50 mL round-bottomed flask. Then the flask was filled with argon and $Pd(PPh_3)_4$ (0.04 mmol, 0.05 g) was added. The resulting mixture was stirred at 80 °C for 30 hours. After the reaction was completed, the mixture was cooled down to room temperature and the solvents were evaporated under reduced pressure. The residue was dissolved in CH_2Cl_2 and extracted with water and brine and dried over anhydrous $MgSO_4$. The solvent was evaporated under reduced pressure, and the crude product was purified on column chromatography on silica gel, eluent: CH_2Cl_2 followed by EtOAc.

T1 (1.7 g, 92 %) as beige solid

^{1}H NMR (400 MHz, $CDCl_3$) δ 8.73 (d, *J* = 2.1 Hz, 4H), 8.68 (d, *J* = 8.0 Hz, 2H), 7.91 – 7.86 (m, 4H), 7.66 – 7.62 (m, 2H), 7.36 (ddd, *J* = 7.5, 4.8, 1.1 Hz, 2H), 3.18 (s, 1H). ^{13}C NMR (101 MHz, $CDCl_3$) δ 156.24, 156.22, 149.43, 149.29, 138.97, 137.02, 132.83, 127.38, 124.04, 122.95, 121.50, 118.85, 83.47, 78.67.

HRMS (ESI): *m*/*z* calcd. for $C_{23}H_{16}N_3$ $[MH]^+$ 334.1344; found 334.1363.

T2 (433 mg, 60 %) as dark yellow oil

^{1}H NMR (400 MHz, $CDCl_3$) δ 8.77 (s, 2H), 8.75 (d, *J* = 4.0 Hz, 2H), 8.69 (d, *J* = 7.9 Hz, 2H), 7.94 (d, *J* = 8.4 Hz, 2H), 7.89 (td, *J* = 7.8, 1.7 Hz, 2H), 7.70 (dd, *J* = 9.7, 5.9 Hz, 4H), 7.57 (d, *J* = 1.2 Hz, 1H), 7.55 (s, 1H), 7.39 – 7.32 (m, 5H), 2.03 – 1.94 (m, 4H), 1.28 – 0.96 (m, 16H), 0.82 (t, *J* = 7.1 Hz, 8H), 0.63 (d, *J* = 7.8 Hz, 6H). ^{13}C NMR (101 MHz, $CDCl_3$) δ 156.02, 155.92, 151.00, 150.79, 149.02, 141.61, 140.36, 137.87, 136.67, 132.06, 130.75, 128.46, 128.34, 127.57, 127.17, 126.91, 125.99, 124.26, 123.75, 122.84, 121.33, 121.24, 120.04, 119.68, 118.46, 92.18, 89.25, 55.13, 40.35, 31.79, 30.02, 29.23, 23.75, 22.60, 14.10.

HRMS (ESI): *m*/*z* calcd. for $C_{52}H_{56}N_3$ $[MH^+]$ 722.4474; found 722.4466.

T3 (256 mg, 55 %) as yellow-orange oil

^{1}H NMR (400 MHz, $CDCl_3$) δ 8.89 (s, 2H), 8.76 (d, *J* = 4.4 Hz, 2H), 8.71 (d, *J* = 7.9 Hz, 2H), 8.05 (d, *J* = 8.2 Hz, 2H), 7.87 – 7.80 (m, 4H), 7.80 – 7.69 (m, 2H), 7.66 (d, *J* = 8.2 Hz, 2H), 7.40 – 7.28 (m, 5H), 2.17 – 1.98 (m, 4H), 1.35 – 1.01 (m, 16H), 0.91 – 0.83 (m, 8H), 0.79 (d, *J* = 4.5 Hz, 6H). ^{13}C NMR (101 MHz, $CDCl_3$) δ 156.24, 155.94, 151.51, 151.03, 149.58, 149.07, 142.25, 140.83, 140.68, 139.15, 137.02, 136.70, 128.82, 127.65, 127.57, 127.03, 126.86, 126.01, 123.73, 122.90, 121.31, 121.27, 120.07, 119.85, 118.57, 55.20, 40.38, 31.79, 30.05, 29.22, 23.85, 22.62, 14.11.

HRMS (ESI): *m*/*z* calcd. for $C_{50}H_{56}N_3$ $[MH]^+$ 698.4474 found 698.4464.

T4 (173 mg, 26 %) as orange solid

^{1}H NMR (400 MHz, $CDCl_3$) δ 8.80 (s, 2H), 8.76 (d, *J* = 3.8 Hz, 2H), 8.69 (dd, *J* = 8.3, 2.7 Hz, 4H), 8.34 (d, *J* = 8.6 Hz, 2H), 8.00 (d, *J* = 8.3 Hz, 2H), 7.89 (dd, *J* = 11.7, 5.1 Hz, 4H), 7.67 – 7.60 (m, 2H), 7.55 (dd, *J* = 11.4, 3.8 Hz, 2H), 7.36 (ddd, *J* = 9.8, 4.9, 2.5 Hz, 2H), 4.23 (t, *J* = 6.6 Hz, 2H), 2.12 – 2.01 (m, 2H), 1.74 – 1.62 (m, 3H), 1.51 – 1.25 (m, 10H), 0.91 (t, *J* = 6.8 Hz, 4H).

^{13}C NMR (101 MHz, $CDCl_3$) δ 156.33, 156.23, 153.02, 149.56, 149.30, 138.29, 137.03, 133.81, 132.20, 127.54, 127.25, 127.00, 125.59, 124.82, 124.72, 124.03, 123.05, 121.54, 118.80, 112.93, 99.84, 88.12, 77.37, 32.06, 30.81, 29.80, 29.76, 29.74, 29.49, 26.37, 22.85, 14.27.

HRMS (ESI): *m*/*z* calcd. for $C_{47}H_{44}N_3O$ [MH^+] 666.3484; found 666.3483.

Measurements: NMR spectra were recorded in $CDCl_3$ with Bruker Advance 400 MHz instruments (for ^{1}H and ^{13}C NMR). High-resolution mass spectrometry (HRMS) measurements were performed using Synapt G2-S mass spectrometer (Waters) equipped with the electrospray ion source and quadrupole-Time-of-flight mass analyzer. Methanol was used as a solvent with the flow rate 100 µl/min. The measurement was performed in positive ion mode with capillary voltage set to 3 kV. The desolvation gas flow was 400 L/h and temperature 150 °C. The sampling cone was set to 20 V and the source temperature was 120 °C. To ensure accurate mass measurements, data were collected in centroid mode and mass was corrected during acquisition using leucine enkephalin solution as an external reference (Lock-SprayTM), which generated reference ion at *m*/*z* 556.2771 Da ($[M + H]^+$) in positive ESI mode. The results of the measurements were processed using the MassLynx 4.1 software (Waters) incorporated with the instrument. Differential Scanning Calorimetry (DSC) was performed with a TA-DSC 2010 apparatus, under nitrogen atmosphere with heating/cooling rate of 20 deg/min. Thermogravimetric analysis (TGA) was recorded using TGA/DSC1 Mettler-Toledo thermal analyzer with a heating rate of 10 ºC/min in a stream of nitrogen.

Spectroscopic Measurements: UV-Vis spectra were recorded using Evolution 300 ThermoFisherScientific spectrophotometer at room temperature in denoted solvents with a conventional 1.0 cm quartz cell. Photoluminescence (PL) spectra in solutions were measured using Hitachi F-2500 Spectrometer. Quantum yields (Φ_f) were estimated using the integrating sphere Avantes AvaSphere-80 with FLS-980 Spectrophotometer (Edinburgh Instruments). Quantum yields were determined by absolute method using the excitation wavelength with the most intense luminescence.

Electrochemical Measurements: Electrochemical measurements were carried out using Eco Chemie Autolab PGSTAT128n potentiostat, glassy carbon electrode (diam. 2 mm), platinum coil and silver wire as working, auxiliary and reference electrode, respectively. Potentials are referenced with respect to ferrocene (Fc), which was used as the internal standard. Cyclic

voltammetry experiments were conducted in a standard one-compartment cell, in CH_2Cl_2 (Carlo Erba, HPLC grade), under argon. 0.2 M Bu_4NPF_6 (Aldrich, 99%) was used as the supporting electrolyte. The concentration of compounds was equal $1.0 \cdot 10^{-6}$ mol/dm^3. Deaeration of the solution was achieved by argon bubbling through the solution for about 10 min before measurement. All electrochemical experiments were carried out under ambient conditions.

Film and blend PVK:PBD on glass preparation: Films and blends in PVK:PBD (50:50 in weight %) were prepared by spin-coating (1000 rpm, 60 s) on a glass substrate from homogenous chloroform solution (10 mg/mL) and dried 5 min in a vacuum oven at 100 ºC.

OLED preparation and EL measurements: Devices with the following sandwich structure configuration ITO/PEDOT:PSS/PVK:PBD:compound/Al with 2 wt. % complex content in blend were prepared. Devices were prepared on OSSILA substrates with pixilated ITO anodes, cleaned by OSSILA procedure recommendation. Substrates were covered with PEDOT:PSS film by spin coating at 5000 rpm for 60 s and annealed for 15 min at 120 °C. Active layer was spin-coated on top of the PEDOT:PSS layer from $CHCl_3$ solution (10 mg/mL) at 1000 rpm for 60 s and annealed for 5 min at 100 °C. Finally Al was vacuum-deposited. J-V characteristic were registered using Keithley SourceMeter. Electroluminescence (EL) spectra were measured with the voltage applied using a precise voltage supply (Gw Instek PSP-405) and the sample was fixed to an XYZ stage. Light from the OLED device was collected through a 30 mm lens, focused on the entrance slit (50 μm) of a monochromator (Shamrock SR-303i) and detected using a CCD detector (Andor iDus 12305). Typical acquisition times were equal to 10 seconds. The pre-alignment of the setup was done using a 405 nm laser.

4. Conclusions

We presented the synthesis and comprehensive characterization of derivatives of 4'-phenyl-2,2':6',2"-terpyridine with ethynyl (**T1**), 2-ethynyl-9,9-dioctylfluorene (**T2**), 9,9-dioctylfluorene (**T3**), 9-ethynyl-10-decyloxyanthracene (**T4**) substituents. Described molecules **T1**-**T4** were prepared by Sonogashira or Suzuki-Miyaura coupling reaction, respectively, with yields between 26 - 92%. Two of obtained molecules are in solid state (**T1**, **T4**), whereas **T2** and **T3** containing fluorene motif are oils. All reported compounds are

soluble and photo- and electroluminescent. **T1** and **T4** are thermally stable, while **T2** and **T3** exhibit significantly lower melting temperature, the temperature of 5% sample weight loss is also lower. **T2** exhibits a bathochromic shift in its absorption and emission spectra and shows higher quantum yield in comparison to **T3**. Obtained data suggest that the acetylene bridge enhances the conjugation of the compound and promotes more efficient energy transfer. It was found that the presence of terminally substituted group, such as alkoxyanthracene via triple bond to 4'-phenyl-2,2':6',2''-terpyridine, significantly modified a wide range of their properties. The introduction of 9-decyloxyanthracene motif increases the PL quantum yield in the solid state in the form of blend with PVK:PBD and EL intensity. Results obtained from electrochemical, optical and DFT studies are consistent, the values of the band gaps are very similar. The results showed that the terpyridines are very promising candidates for the construction of OLEDs.

Acknowledgments

This work was supported by the Ministry of Science and Higher Education, Poland (Diamentowy Grant number 0215/DIA/2015/44).

Calculations have been carried out using resources provided by Wroclaw Centre for Networking and Supercomputing (http://wcss.pl), grant No.18.

Literature

[1] Cargill Thompson AMW. The synthesis of 2,2′:6′,2″-terpyridine ligands — versatile building blocks for supramolecular chemistry. Coord Chem Rev 1997;160:1–52.

[2] Fallahpour RA. Synthesis of 4′-Substituted-2,2′:6′,2″-Terpyridines. Synthesis 2003;2:155-84.

[3] Adrían JC, Hassib L, De Kimpe N, Keppens M. A new approach to symmetric 2,2':6',2'-terpyridines. Tetrahedron 1998;54:2365–70.

[4] Sasabe H, Hayasaka Y, Komatsu R, Nakao K, Kido J. Highly Luminescent π-Conjugated Terpyridine Derivatives Exhibiting Thermally Activated Delayed Fluorescence. Chem - A Eur J 2017;23:114–9.

[5] Cummings SD. Platinum complexes of terpyridine: Synthesis, structure and reactivity. Coord Chem Rev 2009;253:449–78.

[6] Sun Q, Liu W, Shang W, Zhang H, Xue S, Yang W. Improved colorimetric dual-emission and endued piezofluorochromism by inserting a phenyl between 9-anthryl and terpyridine. Dye Pigment 2016;128:124–30.

[7] Karmakar S, Mardanya S, Das S, Baitalik S. Efficient Deep-Blue Emittier and Molecular-Scale Memory Device Based on Dipyridyl–Phenylimidazole–Terpyridine Assembly. J Phys Chem C 2015;119:6793–805.

[8] Zheng M, Tan H, Xie Z, Zhang L, Jing X, Sun Z. Fast Response and High Sensitivity Europium Metal Organic Framework Fluorescent Probe with Chelating Terpyridine Sites for Fe^{3+}. ACS Appl Mater Interfaces 2013;5:1078–83.

[9] Tan J, Li R, Li D, Zhang Q, Li S, Zhou H, et al. Thiophene-based terpyridine and its zinc halide complexes: third-order nonlinear optical properties in the near-infrared region. Dalt Trans 2015;44:1473–82.

[10] Bhowmik S, Ghosh BN, Marjomäki V, Rissanen K. Nanomolar Pyrophosphate Detection in Water and in a Self-Assembled Hydrogel of a Simple Terpyridine-Zn^{2+} Complex. J Am Chem Soc 2014;136:5543–6.

[11] Ozawa H, Yamamoto Y, Kawaguchi H, Shimizu R, Arakawa H. Ruthenium Sensitizers with a Hexylthiophene-Modified Terpyridine Ligand for Dye-Sensitized Solar Cells: Synthesis, Photo- and Electrochemical Properties, and Adsorption Behavior to the TiO_2 Surface. ACS Appl Mater Interfaces 2015;7:3152–61.

[12] Sasaki I. Recent Uses of Kröhnke Methodology: A Short Survey. Synthesis (Stuttg) 2016;48:1974–92.

[13] Tu S, Jia R, Jiang B, Zhang J, Zhang Y, Yao C, et al. Kröhnke reaction in aqueous media: one-pot clean synthesis of 4′-aryl-2,2′:6′,2″-terpyridines. Tetrahedron 2007;63:381–8.

[14] Han FS, Higuchi M, Kurth DG. Diverse Synthesis of Novel Bisterpyridines via Suzuki-Type Cross-Coupling. Organic Letters. 2007;9,4:559–62.

[15] Yuan SC, Chen SB, Zhang Y, Pei J. Rigid Linear and Star-Shaped π-Conjugated 2,2‘:6‘,2‘ ‘-Terpyridine Ligands with Blue Emission. Organic Letters. 2006;8,25:5701–4.

[16] Wu D, Shao T, Men J, Chen X, Gao G. Superaromatic terpyridines based on corannulene responsive to metal ions. Dalt Trans 2014;43:1753–61.

[17] Chakraborty C, Pandey RK, Rana U, Kanao M, Moriyama S, Higuchi M, et al. Geometrically isomeric Pt(ii)/Fe(ii)-based heterometallo-supramolecular polymers with organometallic ligands for electrochromism and the electrochemical switching of Raman scattering. J Mater Chem C 2016;4:9428–37.

[18] Hu Q, Tan Y, Liu M, Yu J, Cui Y, Yang Y. A new highly selective and sensitive fluorescent probe for Zn2+ and its application in cell-imaging. Dye Pigment 2014;107:45–50.

[19] Grosshenny V, Romero FM, Ziessel R. Synthesis, photophysical and electrochemical characterization of terpyridine-functionalized dendritic oligothiophenes and their Ru(II) complexes. J Org Chem. 1997;62,5:1491-500.

[20] Thomas KRJ, Lin JT, Chang C-P, Chuen C-H, Cheng C-C. Zinc(II) and Ruthenium(II) Complexes of Novel Fluorene Substituted Terpyridine Ligands: Synthesis, Spectroscopy and Electrochemistry. J Chinese Chem Soc 2002;49:833–40.

[21] Watanabe Y, Yoshioka R, Sasabe H, Kamata T, Katagiri H, Yokoyama D, et al. Fundamental functions of peripheral and core pyridine rings in a series of bis-terpyridine derivatives for high-performance organic light-emitting devices. J Mater Chem C 2016;4:8980–8.

[22] Liu C-L, Zheng C-J, Liu X-K, Chen Z, Yang J-P, Li F, et al. Multifunctional terpyridine/diphenylamine derivatives as highly efficient blue fluorescent emitters and red phosphorescent hosts. J Mater Chem C 2015;3:1068–76.

[23] Tu S, Li T, Shi F, Fang F, Zhu S, Wei X, et al. An Efficient Improve for the Kröhnke Reaction: One-pot Synthesis of 2,4,6-Triarylpyridines Using Raw Materials under Microwave Irradiation. Chem Lett 2005;34:732–3.

[24] Mishra A, Mena-Osteritz E, Bäuerle P. Synthesis, photophysical and electrochemical characterization of terpyridine-functionalized dendritic oligothiophenes and their Ru(II) complexes. Beilstein J Org Chem 2013;9:866–76.

[25] Aspley CJ, Gareth Williams JA. Palladium-catalysed cross-coupling reactions of ruthenium bis-terpyridyl complexes: strategies for the incorporation and exploitation of boronic acid functionality. New J Chem 2001;25:1136–47.

[26] Goodall W, Wild K, Arm KJ, Williams JAG, Zakeeruddin SM, Humphry-Baker R, et al. The synthesis of 4′-aryl substituted terpyridines by Suzuki cross-coupling reactions: substituent effects on ligand fluorescence. J Chem Soc, Perkin Trans 2 2002;13:1669–81.

[27] Ma X, Jiao J, Yang J, Huang X, Cheng Y, Zhu C. Large stokes shift chiral polymers containing (R,R)-salen-based binuclear boron complex: Synthesis, characterization, and fluorescence properties. Polymer 2012;53:3894–9.

[28] Lee SH, Nakamura T, Tsutsui T. Synthesis and Characterization of Oligo(9,9-dihexyl-2,7-fluorene ethynylene)s: For Application as Blue Light-Emitting Diode. Org. Lett. 2001;3:2005–2007.

[29] Frisch MJ, Trucks GW, Schlegel HB, Scuseria GE, Robb MA, Cheeseman JR, et.al. GAUSSIAN 09 (Revision B.01), Gaussian, Inc. Wallingford, CT; 2010.

[30] Hobert SE, Carney JT, Cummings SD. Synthesis and luminescence properties of platinum(II) complexes of 4′-chloro-2,2′:6′,2″-terpyridine and 4,4′,4″-trichloro-2,2′:6′,2″-terpyridine. Inorganica Chim Acta 2001;318:89–96.

[31] Liu Y, Guo J, Liu R, Wang Q, Jin X, Ma L, et al. Synthesis and luminescent properties of 4'-phenyl-2,2':6',2"-terpyridyl compounds bearing different aryl substituents. J Lumin 2015;157:249–56.

[32] Han F-S, Higuchi M, Kurth DG. Synthesis of π-conjugated, pyridine ring functionalized bis-terpyridines with efficient green, blue, and purple emission. Tetrahedron 2008;64:9108–16.

[33] Fan C, Wang X, Luo J. Blue organic light-emitting diodes based on terpyridine-substituted triphenylamine chromophores. Opt Mater 2017;64:489-495

[34] Bujak P, Kulszewicz-Bajer I, Zagorska M, Maurel V, Wielgus I, Pron A, et al. Polymers for electronics and spintronics. Chem Soc Rev 2013;42:8895.